6. INSTRUMENTATION

Isidore Warshawsky

An industrial power generating and transmitting system uses a variety of instrumentation to monitor and control the system. The principal demands made on the instrumentation system are that there exist a proper balance between accuracy and reliability and an adequate capacity for growth to accommodate future needs.

The means for meeting these demands are hardware, operational techniques, and the systems management that blends all ingredients into a consistent, effective instrumentation system. The hardware comprises tangible items like sensors, recorders, and intermediate components. The operational techniques include not only the installation and use of the hardware, but also the manipulation, analysis, and interpretation of the data.

A great amount and variety of instrument hardware already exists to form the building blocks of any instrumentation system. The Transducer Compendium published by the Instrument Society of America (ISA) lists over a thousand models of commercially available sensors. A commercial directory of electronic instruments lists over 10 000 models of instruments other than sensors. Consequently, modern industrial and aerospace instrumentation development is concerned even more with new techniques of using existing hardware - and of improving old techniques - than with hardware development. Nevertheless, both hardware and techniques are subjects of current research. This paper will give some specific examples of both. These examples are sometimes relevant to the advanced concepts presented in other papers of this conference and sometimes relevant to present-day systems. Some criteria for effective instrument systems management will also be discussed.

SENSORS, TECHNIQUES, AND THEIR COMBINATIONS

Liquid-Metal Pressure Measurement

A majority of the more than 300 pressure transducers listed in the ISA compendium are of the aerospace type. Some of the distinctive characteristics found in these are

(1) small size (e.g., 3- or 6-mm diameter cylinders; 1-mm thick disk)
(2) high output (e.g., 5 V because of built-in amplifiers or because of rheostat-potentiometer design)
(3) vibration resistance
(4) nuclear-radiation resistance
(5) 250° C (~500° F) operation

Several of these characteristics may sometimes be found in the same sensor.

Some of the transducers capable of operating at 250° C may be used to measure gage, absolute, or differential pressure in a liquid-metal system. The manner in which one leg of such a transducer might be connected to a pipe containing liquid metal is shown in figure 6-1. Connecting tubes slope for drainage. Heaters are used to preheat the system in preparation for receiving the metal and for keeping it liquid thereafter.

When the liquid is sodium or a sodium alloy, the oxide of sodium tends to collect as a precipitate in the coolest part of the system. In order to prevent such precipitation from clogging the connecting tubing, a trap is provided and cooled as shown in the figure, so that the oxide will preferentially collect in the trap, where it may be drained off occasionally.

Transducers operating continuously at elevated temperature may suffer a zero shift of a few percent in a few months. If such shift exists and is intolerable and if periodic recheck of the zero is impossible, one of the arrangements shown in figure 6-2 may be preferred. Here, the transducer is at room temperature, and a slack diaphragm, operating at elevated temperature, isolates the liquid metal. The slack diaphragm transmits pressure or force with negligible resistance. In figure 6-2(a), pressure is transmitted through a NaK eutectic which remains liquid even at room temperature. This eutectic completely fills the volume between the slack diaphragm and the spring diaphragm of the transducer. Such a pressure-measuring assembly, although bulky and expensive, has proved accurate and reliable. In figure 6-2(b), force is transmitted to the tranducer spring through a long stainless-steel rod or tube, which is gas cooled to sustain the temperature gradient. Both of the arrangements shown in figure 6-2 are available commercially.

NASA-Lewis experience is now sufficient to ensure reliability of construction of systems like those shown in figures 6-1 and 6-2. This reliability derives from the ability to maintain adequate purity of the liquids, the containment material, and the purging and cover gases, and to make reliable welds without introducing oxygen contamination.

Electromagnetic Flow Metering

The electromagnetic flowmeter's advantages of obstructionless flow and negligible pressure loss favor it for liquid-metal flow measurement. The principle of the flowmeter (fig. 6-3(a)) is Faraday's Law, which states that, when a material flows at velocity V transverse to a magnetic field of flux density B, a potential gradient E/L is generated that is proportional to the vector cross product of B and V.

Flowmeters based on this principle have been used in oceanography, medicine, and rocket research. Flowmeters are currently available commercially, from many suppliers, for measuring the flow of weak or strong electrolytes. Pipe sizes range from 3 millimeters to over 1 meter. The standard units use a 60-hertz magnetic field in order to suppress polarization voltages at the electrodes. The conventional configuration is that of figure 6-3(c), wherein two metallic pins project through the wall of an insulating pipe to serve as electrodes; the leads from these pins must be dressed very carefully and symmetrically in order to prevent hum pickup that might otherwise obscure the Faraday effect signal.

In a liquid-metal application, there is no polarization; hence, a dc magnetic field may be used with a permanent magnet as a convenient source, and careful dressing of leads is not required. Figure 6-4 shows such a flowmeter. It is of 1/2-inch size, with a swaged guard heater to prepare it for accepting the metal and keeping it liquid thereafter. The large-diameter enclosures around the central tube are thermal insulation.

Two unusual consequences result from the high electrical conductivity of liquid sodium or potassium. First, the containment tube may be made of stainless steel, with electrode leads welded to the outside of the tube, thus maintaining high mechanical reliability (fig. 6-3(b)). The correction to the basic Faraday Law formula for the nonzero conductivity of the stainless steel is known accurately. Second, circulating fluid currents are induced, of the form shown in figure 6-3(b), that destroy the axial symmetry of velocity on which the basic formula is predicated. The resultant error may be as high as 4 percent, in a practical case; however, under a recent NASA-university contract, the error has been computed well enough so that resultant inaccuracy after the correction has been applied is less than 1 percent. After adding errors from other sources, the overall probable error of flow measurement may be no more than 2 percent.

The flowmeter may also be used with nonpolar, nonconducting fluids if the magnetic field is of relatively high frequency, say, 1 to 10 kilohertz, and the electrodes are capacitor plates (fig. 6-3(d)). The flow of lubricating and transformer oils has been measured successfully; commercial meters for this purpose may be available in another year. An NASA contract for developing a similar flowmeter for liquid

hydrogen has already produced a prototype that confirms the feasibility of such a measurement.

Temperature Measurement by Infrared Radiation

The development of infrared-sensitive devices, stimulated largely by military interest over the past 25 years, has resulted in many diverse applications of infrared photography and radiometry. Thus, infrared photographs from a satellite have distinguished over a dozen different types of vegetation and crops, and an aerial photograph of a citrus orchard can distinguish between healthy trees and those infected with insect scale, because the latter trees appear darker. In medicine, local regions of infection near the surface of the body are revealed by infrared photography because such infected regions are slightly warmer. The U. S. Air Force, in its research on arctic clothing, has taken time-lapse photographs of a man entering a refrigerated chamber, to observe the relative rates of cooling of different parts of the body. Such photographs confirm that skin areas of reduced circulation, like those covering most bony surfaces, are the first to feel the chill.

Boiler inspection. - Figure 6-5 shows the side of a boiler, including a door, as photographed by ordinary light and by infrared. A suspected heat leak around the edge of the door was confirmed by the infrared photograph, which showed a leak at the left edge of the door, but the photograph also revealed that the insulation behind an adjacent wall panel had failed. Such an advance finding reduced the subsequent downtime when the boiler was shut down for maintenance. Temperatures of some of the surfaces may be estimated by comparing image brightness in the infrared photograph with the brightness of the rectangles that appear in the strip at the top of that photograph. These rectangles represent strips of metal held at known temperature; in this photograph, the temperatures range between 60° and 250° C (140° and 500° F).

Jet-engine-turbine pyrometry. - Figure 6-6 shows a jet-engine turbine-rotor-blade pyrometer for flight use. This instrument, developed in England, uses a silicon photocell, may be fuel-cooled or air-cooled, is temperature compensated and vibration resistant, and has successfully undergone over 300 hours of actual engine operation.

The method of installation is shown in figure 6-7. The instrument sights between the stator blades, at an area on the rotor blade that is about 1 centimeter in diameter and about halfway between root and tip of the blade. Location and size of the area of view may be altered by changing the angle of sight or the viewing distance, respectively. However, the direction of sight is always controlled so that the

instrument may not see past the rotor. Thus, the photocell output represents some average temperature of the blade surfaces passing the line of sight. The photocell output more nearly represents actual blade temperature because (1) the space between adjacent stator blades resembles a blackbody cavity to a modest degree and (2) the spectral bandwidth of effective radiation is quite narrow because of the photocell's spectral characteristic; thereby, the dependence of radiant flux on blade-surface emittance is minimized.

The photocell can respond to radiation in only a few microseconds. Consequently, the passage of a single overheated blade is detectable, in laboratory tests, when photocell output is observed on a synchronized oscilloscope. This feature is useful in turbine-cooling research, where a rotor may contain only a few special test blades.

Mapping of blade temperature distribution. - At Lewis, NASA has used infrared to map temperature distribution on the surface of a stationary turbine blade under test in a high-temperature wind tunnel. As indicated in figure 6-8, the surface is photographed on infrared-sensitive film. Hotter areas produce brighter images, but the association of image brightness (more accurately, photographic-image density) with actual temperature requires several intermediate steps. Image density depends on the photographic-development process and on the intensity of radiation emitted by the surface. The latter quantity, for a surface of given temperature, depends on the emittance of the surface which, in turn, is determined by

(1) surface material

(2) surface roughness

(3) surface geometry

(The intensity of radiation also depends on the geometry and emittances of contiguous surfaces, but their effects can be made small in these controlled experiments.) Dependence on emittance may be minimized by using a narrow spectral bandwidth. The filter (fig. 6-8) and the spectral limitation of the infrared-sensitive film itself together define the upper and lower limits of the spectral band that provides the best compromise between sensitivity and emittance dependance. Thereby, a 10-percent uncertainty in emittance produces less than 1-percent uncertainty in temperature.

The more direct way to allow for the photographic development process is shown at the bottom of figure 6-8. A strip of turbine-blade material, of uniform cross section, is clamped between two massive blocks at known temperatures T_1 and T_2. Then, there is a linear temperature gradient in the strip. If photographs of this strip and of the blade under observation are taken on similar pieces of film, and both photographs are processed through the same developer at the same time, a match of optical densities on the two pieces of film will yield the corresponding temperatures.

A less direct, but more convenient and more accurate method of allowing for the photographic development process is shown in the middle view in figure 6-8. This method does not require the construction and maintenance of a heated temperature standard. In this alternative approach, a commercially available film strip, divided into areas of progressively higher transparency, is photographed while uniformly illuminated as shown in the figure. The relative transparencies of the areas are known accurately; hence, the relative intensities of radiation forming the photographic image are also known accurately. If photographs of the blade and the illuminated strip are taken on the same roll of film and then developed together, a match of densities on the two photographs yields the corresponding relative intensities of radiation emitted from various areas of the test blade. To obtain the final conversion to absolute temperature, a single thermocouple is installed at one point on the blade. The actual temperature corresponding to the photographic density at this point now being known, the temperatures corresponding to other densities also become known.

Figure 6-9 contains photographs of a typical heated blade and of a calibrating strip. The installed thermocouple may also be seen (there are several in the photograph, but only one is relevant to the present discussion). Since figure 6-9 represents a photographic negative, blacker areas represent hotter areas.

The corresponding contour lines of constant density are shown in figure 6-10, as well as the approximate values of corresponding temperature. The detailed interpretation of all that appears in figure 6-10 is beyond the scope of this paper; it suffices to note that, after the successive conversion from relative photographic density, to relative radiant intensity, to relative temperature (from Planck's radiation law), to absolute temperature, temperature differences of 10° F ($\sim 5^{\circ}$ C) are detectable.

To measure temperature of a moving rotor blade rather than of a stationary one, the camera of figure 6-9 is replaced by an image converter tube, as shown in figure 6-11. These tubes are similar to those used in military sniperscopes or snooperscopes. Since their operation depends on the presence of certain electrode voltages, the application of these voltages may be synchronized with the passage of a rotor blade past a fixed point on the turbine casing, to provide a stroboscopic effect. The image formed by the image converter tube may be photographed with an ordinary camera. The same image converter must be used to observe any calibration standards used. This technique is currently under development at Lewis and has not yet been proved to yield accuracies or sensitivities commensurate with those obtained by direct photography of stationary blades.

The problem of rotor-blade temperature measurement will be treated later, in the section Rotating-Shaft Data Transmission.

Potential Applications. - The availability of image converters suggests other applications of infrared. Observation with a snooperscope in the field might permit visual detection of overheated components of generating or distribution equipment. Figure 6-12, although taken directly with an infrared camera rather than through a snooperscope, illustrates such a potential application. Three distribution transformers on a utility pole are shown to be equally loaded. The low-voltage feeder from them is also noticeable. The utility pole also appears warm because it has been heated by sunlight and because its infrared emittance and absorptance are very high. Comparison with the reference scale at the top of the photograph would confirm that the transformers are operating within acceptable temperature limits. However, such a scale, calibrated to simulate metal objects, would ordinarily not be quantitatively correct for nonmetallic materials of considerably higher emittance.

Rotating-Shaft Torque Measurement

Research on high-speed pumps and turbines for cryogenic liquids has required the development of a shaft torquemeter capable of operating at shaft speeds up to 50 000 rpm. The optical torquemeter developed for this purpose obviously has wider application than this original use.

As shown in figure 6-13, a special torsional spring element is fabricated in the form of a shaft with polished reflecting surfaces at each end. An even number of surfaces is generally used at each end, to facilitate mechanical balance. A stationary optical unit measures twist of the shaft, independent of moderate translation between the stationary unit and the rotating shaft.

The optical system projects the illuminated image of a slit, by successive reflection from each of the reflecting surfaces on the shaft, on to two photocells separated by a hairline gap. Shaft twist produces unbalanced illumination on the two photocells. A servomechanism thereupon repositions the photocells to restore the null-balance condition. Photocell position is a measure of shaft twist.

If a laser is used as the slit illuminant, the resultant higher intrinsic slit brightness, with its consequent higher signal-to-noise ratio, yields higher accuracy.

Figure 6-14 shows torquemeter shafts having full-scale ranges of 2, 400, and 1200 foot-pounds, respectively. Inaccuracies of one percent or less have been obtained regularly.

When a very large shaft is involved, the manufacture of a special torsional element with its reflectors becomes very expensive. The alternative arrangement shown in figure 6-15 may then be usable. If a shaft is already available that is operating well within its proportional limit, so that it is a good spring, and if several

diameters of straight length of shaft are accessible, separate rings carrying mirrors may be clamped on to the shaft. Each ring is split and doweled to permit its installation without dismantling the machine. Diameters must be matched and concentricities maintained well enough to assure accurate balance. The distance between clamping planes constitutes the "gage length" of the spring. Calibration may be computed if shaft dimensions and shear modulus are known accurately enough. Otherwise, empirical calibration must be performed by clamping the shaft well outside the gage length and applying a known torque with hydraulic pistons; this torque need be only a small fraction of full-scale torque if the shaft is used well below its proportional limit and if there is adequate sensitivity.

Computations indicate that this sensitivity requirement can be met if a laser illuminant is used and if there is a multiplicity of mirrors, as shown in figure 6-15. A further advantage of using many mirrors is that standing torsional oscillations are averaged.

Bulk-Velocity Measurement with Pitot Tubes

This section will present a number of techniques associated with the application of the pitot tube to the measurement of bulk velocity in ducts or pipes. The techniques are not necessarily related; in fact, some are contradictory, but each is useful on some occasion.

Velocity measurement in smooth pipes. - The bulk velocity of a fluid flowing through a long, straight, round pipe with smooth walls may be deduced from a single measurement of linear velocity at the center of the pipe, as may be provided with the pitot tube shown in figure 6-16, because the velocity profile is well defined. The dependence on Reynolds number is no stronger than that of an orifice or venturi, but the pitot tube provides the advantages of smaller expense, negligible pressure loss, and freedom from the need for maintaining sharp edges or very clean surfaces. If line pressure is high, conventional engineering practice will lead to a correspondingly high differential pressure; then, if the fluid is primarily gaseous, even the presence of small amounts of liquid in the pressure line will not affect the differential-pressure measurement appreciably.

The static-pressure tap is a more likely source of error than the total-head tube. The tap in the side wall must be accurately flush and square, the wall itself must be smooth, and there must be no downstream obstruction nearby; the pitot tube is shown cantilevered for this last reason, although the supporting strut could have extended across the pipe if the wall tap had been located 90^{o} away from the plane of section.

Velocity measurement in large ducts. - Bulk velocity in a duct so large that the velocity profile is uncertain and use of an orifice is uneconomical may be obtained by integration over the cross section. The pitot tube of figure 6-16 may be traversed continuously across the duct. Alternatively, a fixed rake of appropriately located pitot tubes may be installed, so that the sum of the total-head readings will yield the bulk velocity (fig. 6-17). In the latter case, the summation may be performed automatically if each total-head tube is connected through an identical flow impedance to a common plenum. The flow impedance, as shown in the detailed sketch of figure 6-17, might be a capillary 1/2 millimeter in diameter by 1/2 meter long. Identity of all impedances may be assured by cutting all the individual capillaries from the same piece of capillary tubing and locating all impedances at the same place so that they will all be at the same temperature. Danger of clogging the capillaries is minimized if the following conditions are met: (1) entrance ends of the capillaries are shaped to promote inertial separation of occasional droplets or solid particles, (2) capillaries are located at the common-plenum end of the connecting tubes, (3) these tubes are relatively long and of comparatively large diameter, (4) rates of increase of line pressure and velocity head are slow enough that entrainment velocities are low. Obviously, however, the capillaries cannot be used in an intrinsically dirty fluid.

The associated static-pressure measurement may use one of the techniques shown in figure 6-18. The more straightforward approach is to install a wall tap at 90^{o} from the line of total-head tubes and in the plane of their mouths (fig. 6-18(b)). This approach may fail if the duct wall is so rough that one of the conditions for reliable static-pressure measurement is violated. Then, the necessary alternative is to mount a static-pressure measuring probe on the strut carrying the total-head probes (fig. 6-18(a)). This probe may be on the centerline of the duct, with static-pressure sensing holes on the side of the probe, in the plane of the mouths of the total-head tubes. The distance from this plane to the leading edge of the supporting strut should be greater, in this case, than would be necessary in the case of figure 6-18(b), in order to minimize the interfering effect of the strut. Nevertheless, this interference is appreciable and must be corrected for. The magnitude of the correction was determined at this Center many years ago and is known with sufficient accuracy to permit reliable bulk velocity measurement.

Inertial separation of droplets. - Figure 6-19(a) illustrates how total pressure may be measured in a gas stream containing entrained droplets of liquid and how clogging of the connecting tube may be avoided. This connecting tube extends downward into the pitot tube and is beveled to minimize droplet adhesion. The higher inertia of the droplets causes them to impinge on the rear surface where they are decelerated and drain through the bleed hole. This principle is used in all airspeed

heads for airplanes, which, of course, must fly through rain.

Figure 6-19(b) shows how placing the static-pressure-sensing holes behind a step may promote inertial separation of droplets. The presence of the step causes an appreciable error in static-pressure indication, but this error is reproducible, may be determined by calibration, and hence may be applied as a correction. This technique has been used in our icing-research measurements.

Measurement when particulate matter is present. - No always-reliable method exists for pressure measurement in a "dirty" gas stream. However, the following expedients have been helpful at one time or another.

(1) In applications where only an occasional measurement is required (e.g., a 10-sec reading every 10 min), a probe may be retracted for the time between readings, or else shielded against impact of the fluid.

(2) Using a probe of maximum tolerable diameter may reduce the frequency with which it must be cleaned.

(3) A flush-diaphragm miniature pickup may be mounted at the mouth of a total-head tube, or flush with the pipe wall to measure static pressure, provided ambient temperature conditions permit such installations. In total-head measurement, there should be sufficient overrange capability to handle an occasional particle of above-average kinetic energy. Build-up of dry particles at the nose ordinarily will not appreciably affect the integration of total pressure unless cementing occurs, so that diaphragm stiffness is altered.

(4) Reverse flushing with clean gas, often suggested, is ineffective unless the flushing gas is moving at high velocity. Elaborate precautions are required to prevent damaging the transducer during the flushing operation. This technique is applicable when sampling is acceptable, as in expedient (1).

Integration by Sampling

The technique to be discussed in this section is applicable to the integration of any physical quantity, such as pressure, temperature, flowrate, or composition, over an area of any shape. However, to simplify the discussion, it will be assumed specifically that the average pressure over a circular area is to be determined with an integrating rake like that in figure 6-17.

In order that the sum of the pressures measured by the individual tubes shall yield the average pressure, conventional mechanical engineering practice has been to divide the circular area into annuli of equal area and to locate a sampling probe at the center of gravity of each annulus (fig. 6-20(a)). If three stations are used on each side of the centerline, the error in average pressure yielded by summing the

individual readings will be from 1 to 3 percent, depending on the shape of the pressure profile.

The error would be reduced if the pressures were plotted against radius, a smooth curve drawn through the points, and the integral corresponding to this curve then determined (fig. 6-20(b)). This error would be smaller than that produced by the bar-graph summation of figure 6-20(a) because an additional item of intelligence is used: that the pressure distribution is smooth.

The operations of curve drawing and integration need not be performed literally, because a mathematically identical result can be performed by the mere addition of pressure readings, as in the original procedure, provided the measuring stations are at locations slightly different from those of figure 6-20(a). These revised locations are listed in table 6-I.

This integration technique is termed Chebyshev integration. It generally produces an error less than one tenth of the error obtained with the centroid-of-equal-areas method.

Rate Indication

In some engineering operations, knowledge of the rate of change of a physical quantity is even more important than knowledge of the absolute value of that quantity. Direct measurement and indication of this rate is then desirable. For specificity, assume that the rate of rise of turbine-nozzle-block temperature is to be monitored during turbine startup. If the temperature sensor is a thermocouple or resistance thermometer bulb, its output may be delivered to a resistance-capacitance differentiating network (fig. 6-21(a)) or to a resistance-inductance differentiating network. In the latter case, the inductor may be the primary of a step-up transformer, as in figure 6-21(b); the output voltage is thereby increased, but at the expense of a higher output impedance. Either circuit requires an amplifier of constant gain, because available output power is low. A further improvement is therefore achieved by using an operational amplifier, as in figure 6-21(c), so that amplifier gain stability is not required. The circuit of figure 6-21(c) uses the same differentiating components, R and C, as that of figure 6-21(a). However, if the rate of change of input voltage is very low, an additional resistor R' and capacitor C' must be included to inhibit the ability to differentiate higher-frequency components, such as powerline hum, whose derivative would otherwise mask the rate indication of interest.

Using resistors, capacitors, and an amplifier of sufficiently high quality, a rate of change of temperature of 200° C per hour may be measured reliably.

Time-Lag Compensation

The circuits of figure 6-21 are readily converted to lag-compensating circuits (fig. 6-22) by providing a dc path that adds the input signal to the derivative signal in appropriate proportions. Such lag compensation is particularly useful in control applications because it helps to avoid overshoot of the variable being controlled.

Time lag compensation concepts are illustrated in figure 6-23. Again, for specificity, the variable will be assumed to be temperature, because long time lag is most commonly associated with this variable.

If an abrupt, step-like change in temperature, shown by the heavy line, is imposed on a thermally massive object, the temperature of the object will rise slowly, as shown by the curve marked "original". A tangent to this curve at the origin will intersect the asymptote of the curve at a time termed the "thermal time constant" of the object.

Interposition of a lag-compensating circuit between sensor output and indicator will result in an indication that follows the curve marked "compensated", which has an equivalent time constant considerably shorter than that of the original object. Proper compensation is achieved when the electrical time constant of the basic differentiating network of figure 6-21, as used in figure 6-22, is equal to the thermal time constant of the object.

If electrical and thermal time constants are not matched, undercompensated or overcompensated responses are obtained, as shown by the dashed curves of figure 6-23. In either case, there is an improvement in response. However, in some control applications it may be necessary to avoid the overshoot associated with the overcompensated case.

Reductions in response time of 10 to 100 times have been obtained routinely. Principal applications have been in thermometry and hot-wire anemometry.

Rotating-Shaft Data Transmission

The transmission of electrical signals to and from rotating members has conventionally been performed through slip rings. This approach is troublesome where a high-speed system like a jet engine rotor is being studied, because considerable maintenance and careful manipulation are required to assure reliability. NASA-Lewis currently is developing an alternative telemetering approach; it is illustrated in figure 6-24.

Thermocouple leads from the turbine rotor are run radially to the center of the shaft, which is hollow, and then to the front end of the shaft. Pressure taps on the

compressor rotor are connected by radial tubes to miniature transducers mounted near the center of the shaft, and the electrical leads are also run to the front end of the shaft; the electrical-signal transmitting unit is mounted here because this region may be kept cool with relative ease.

Electrical signals are transmitted through a standard commercial rotating transformer. This unit has several pairs of stator and rotor windings that act like primary and secondary windings of a transformer. Each pair of windings is electrically and magnetically isolated from the others. Signals from 100 hertz to 1 megahertz can be transmitted with negligible modulation at the frequency of shaft rotation. The ball-bearing-supported rotor is coaxial with the main engine shaft and rigidly attached to it; only two semiflexible arms, attached to the engine nacelle and the stator casing, are needed to keep the latter from rotating.

An assembly of four printed-circuit boards, contained in a 10-centimeter-diameter by 10-centimeter-long can, is attached to the rotor and turns with it. This assembly contains solid-state circuitry for switching electrical signals, amplifying them, and converting them into digital form.

The block diagram of the system is shown in figure 6-25. Power enters through one channel of the rotating transformer in the form of 10-kilohertz square waves. This frequency is also used to define the clock frequency for the subsequent digitization. The incoming power is changed on a power converter board into dc power for operating the electronics and the pressure transducers. Outputs from the pressure transducers and thermocouples pass to a multiplexer board, which acts as a 2-pole, 36-position switch. Channel switching occurs 50 to 100 times per second. The multiplexer output is converted on a third board into a digitized, pulse-code-modulated form, leaving through a second channel of the rotating transformer as pulses of 5-volt amplitude. Effects of noise and hum at the output are therefore negligible.

Figure 6-26 shows the system hardware. The rotating transformer is at the center of the photograph. Clockwise from the upper left-hand corner are the power-converter, multiplexer, and digitizer boards, and a board containing amplifiers and other circuitry for controlling the sequence of electronic operations. Although individual components have been proved to operate satisfactorily at rotational speeds corresponding to 10 000 g at the rim of the boards, the assembly of the prototype has not yet been completed. If environmental tests are passed, an inaccuracy of less than 0.5 percent of full scale should be attained.

SYSTEMS MANAGEMENT

Effective instrument systems management starts in the conceptual stage of a new plant design with a definition of the ultimate goals of the system. This first step is also the one step that transcends any mathematical or mechanistic analysis because it requires knowledge of engineering, economics, and public relations, and relies on experience, imagination, and vision. It must be performed at the highest level of management.

Subsequent management steps involve the translation of the basic goals into a system of hardware and defined operational procedures that will provide adaptability to changing needs, capacity for growth, and acceptable accuracy and reliability.

The advance specification and provision of features that have only a modest probability of subsequent use may constitute a sound insurance investment against the risk of having to add such features after a machine is built. Similarly, the cost of initial installation of features that may permit later automatization may be only a small fraction of the cost of their subsequent installation. Examples related to material presented in this and the preceding two papers of these proceedings are (1) specifying a hollow shaft for possible later installation of data transmission leads, (2) providing sufficient straight length of coupling shaft to allow subsequent torque measurement, (3) inclusion of ports for later insertion of probes, sighting tubes, or other diagnostic devices, (4) provision of checking terminals and pressure ports, and (5) addition of duplicate connections or ports for subsequent redundant connections that may improve reliability or expedite automation.

After full definition of the techniques of using the designated hardware and facilities, procurement of hardware may be initiated. Such procurement requires that the user, rather than the supplier, have the responsibility for correct specification.

At this Center, for each hardware item, such as a transducer, the following steps are taken.

(1) Every relevant performance item is specified, by stating, for each item, the acceptable limit of error, and the exact test method that will be used for checking that item. Construction features that affect reliability are also specified in concrete terms of performance. No performance item is specified that cannot be checked.

(2) The specification on each item is realistic. A common check is that the specification on each item is met by at least two manufacturers with their standard advertised equipment. Performance is specified (as the user requires it) rather than design, which is best left to the manufacturer.

(3) Specifications are rigorous; highest quality of performance is required. The premium paid for this quality is negligible compared with the cost of losing a single run because of inferior quality.

(4) Once specifications are established, award is made to the lowest bidder who meets all specifications.

(5) Each item is inspected and tested for each performance item specified, except where there is strong statistical evidence that some test need be performed only on samples.

The specific performance items characterizing a differential-pressure transducer of the type used to measure fluid velocity in a pipe are shown in the following list:

Sensitivity accuracy at standard conditions Sensitivity change with temperature Sensitivity change with time Hysteresis at midscale Repeatability for unidirectional approach Nonlinearity	Zero adjustment reproducibility Zero shift with line pressure Zero shift with mounting strain Zero shift with acceleration Zero shift with temperature
Full-scale-output change with supply pressure Full-scale-output change with line voltage Full-scale-output change with acceleration	Zero shift after overrange Hysteresis at zero Zero drift with time Zero shift after cycling
Range Sensitivity (transduction factor) Overrange protection Maximum line pressure Maximum ambient temperature Minimum ambient temperature Weather protection Power supply (line) voltage Line frequency Power supply (input) pressure Mounting	Source impedance Load impedance effect Line resistance effect Insulation resistance to ground Common mode rejection
	Chamber volumes Chamber volume change for full-scale ΔP Damping Natural frequency
	Pressure connections Vent or bleed connections Filter Zero adjustment accessibility

A more general list of items that might be associated with the installation of such a transducer is

Channel identification	Positioning
Electrical continuity	Alinement
Electrical polarity	Vibration isolation
Insulation resistance	Strain relief
Line and connector resistance	Weatherproofing
Cable dressing	Nonflamability
Grounding	Heat dissipation
Electrostatic shielding	Materials compatibility
Electromagnetic shielding	Lubrication
Transposition	Internal cleanliness
Crosstalk	Pressure tightness
Shunt capacitance	Vacuum tightness
Impedance balance	Thermal insulation
Checking terminals	Accessibility for maintenance
	Isolation for inspection

For every hardware component, subsystem, and system, the operations of qualification and checkout, as discussed in depth in papers 4 and 5 of this conference, are essential to ensure reliability. Nor can this reliability be maintained unless there is periodic maintenance and recheck of all system elements.

Finally, continued maintenance of operating economy and retention of competitive advantages requires periodic review and updating, to take advantage of modern developments.

TABLE 6-I. - STATION LOCATIONS FOR

SMOOTHED AREAL AVERAGING

IN CIRCULAR DUCT

Number of stations along one radius	Radial locations, fraction of duct radius
2	0.4597, 0.8881
3	0.3827, 0.7071, 0.9239
4	0.3203, 0.6382, 0.7699, 0.9473

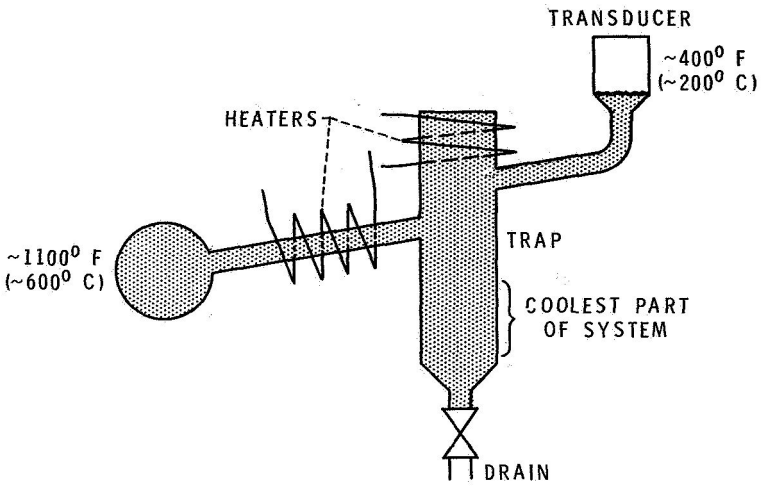

Figure 6-1. - Liquid-metal pressure measurement. Transducer at elevated temperature.

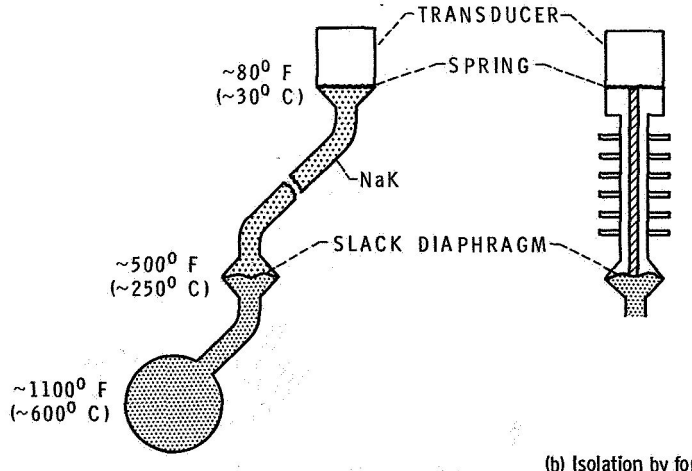

(a) Isolation by pressure transmission.

(b) Isolation by force transmission.

Figure 6-2. - Liquid-metal pressure measurement. Transducer at room temperature.

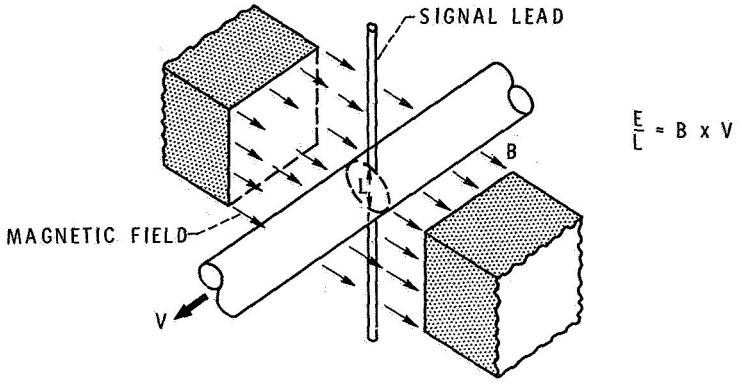

(a) Principle.

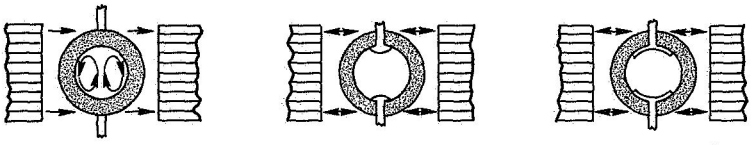

(b) Liquid metals. (c) Electrolytes. (d) Dielectric liquids.

Figure 6-3. - Electromagnetic flowmeters.

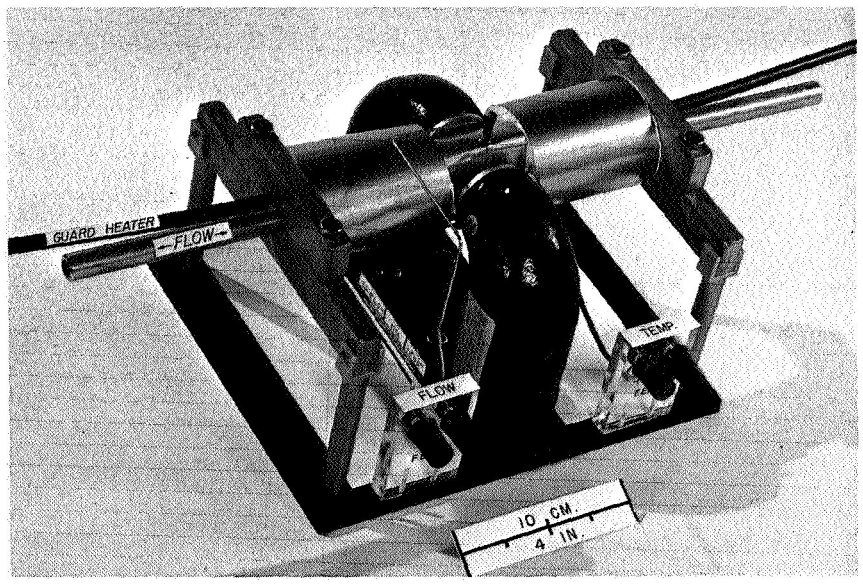

CS-47662

Figure 6-4. - Electromagnetic flowmeter for liquid metals.

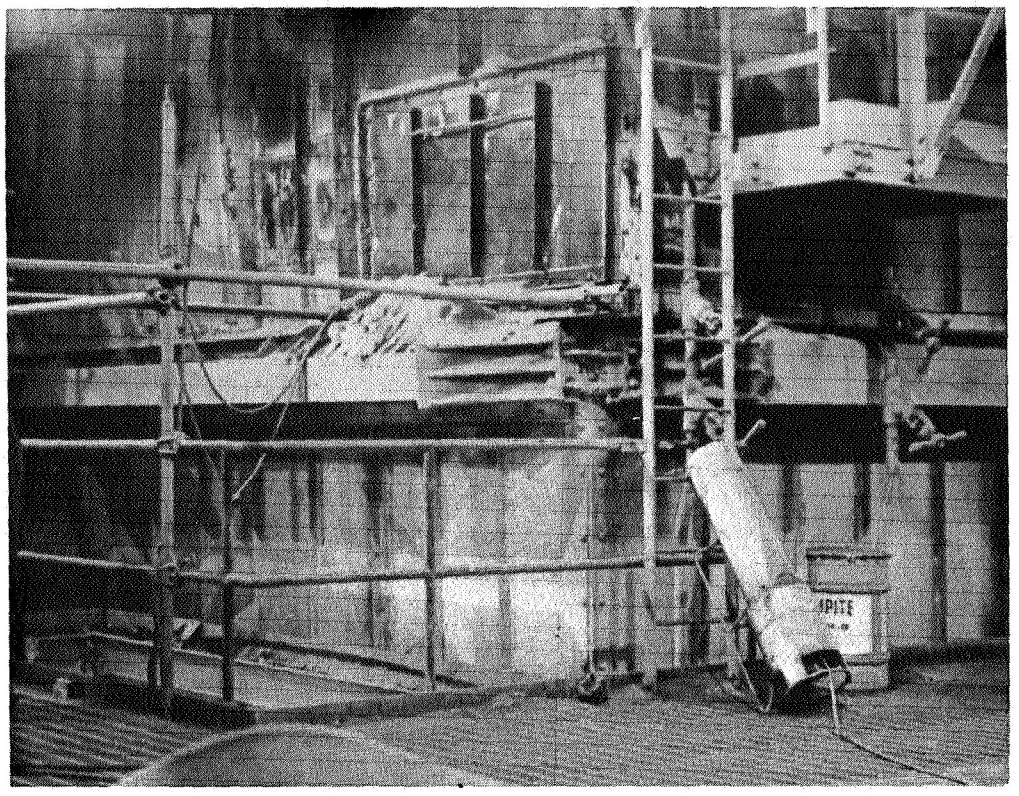

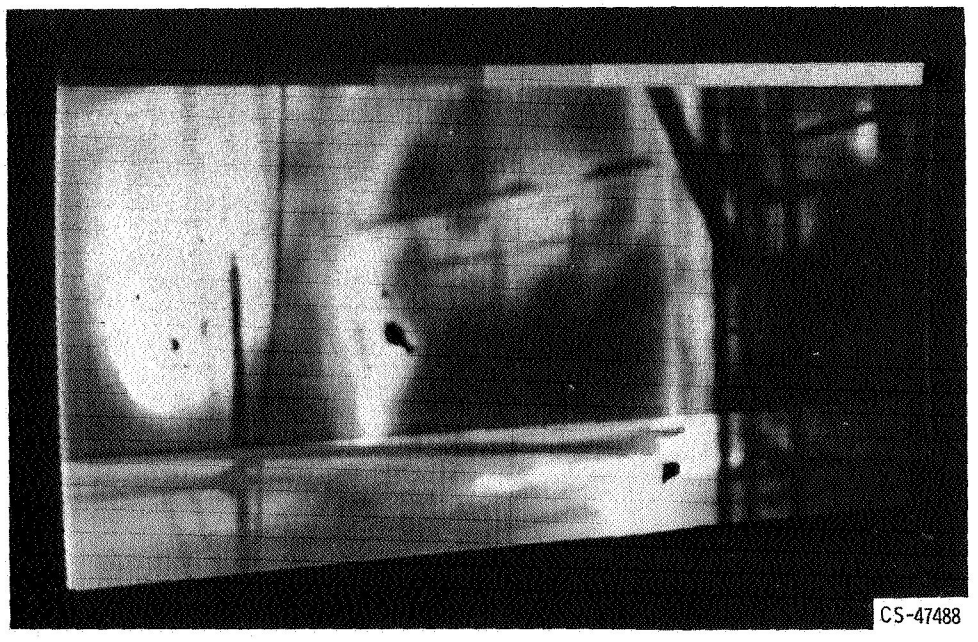

Figure 6-5. - Boiler door. Gray scale temperatures: 140°, 160°, 183°, 214°, 262°, 300°, 380°, and 500° F. (Courtesy Barnes Engineering Co.)

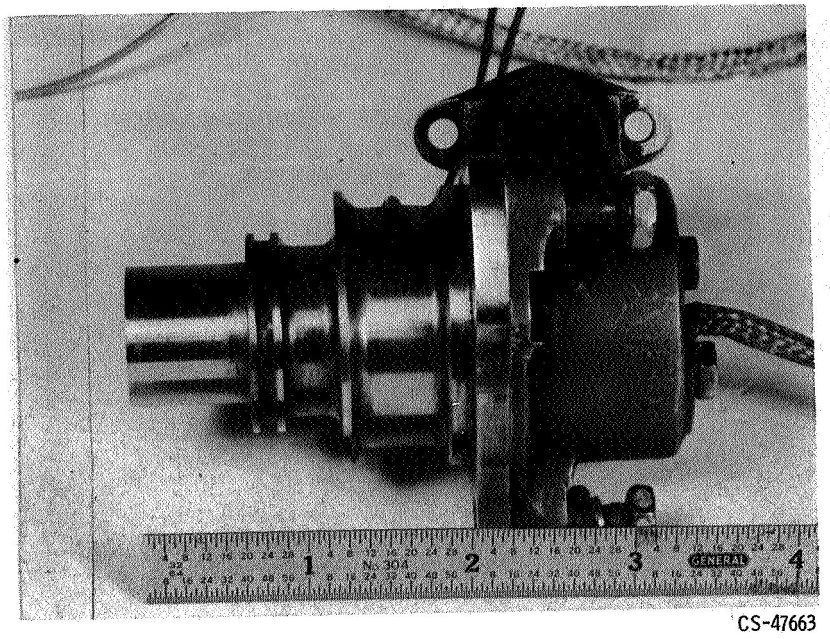

Figure 6-6. - Turbine-blade pyrometer for jet engine. (Courtesy Land/ Electro-nite Co. and Rolls Royce, Ltd.)

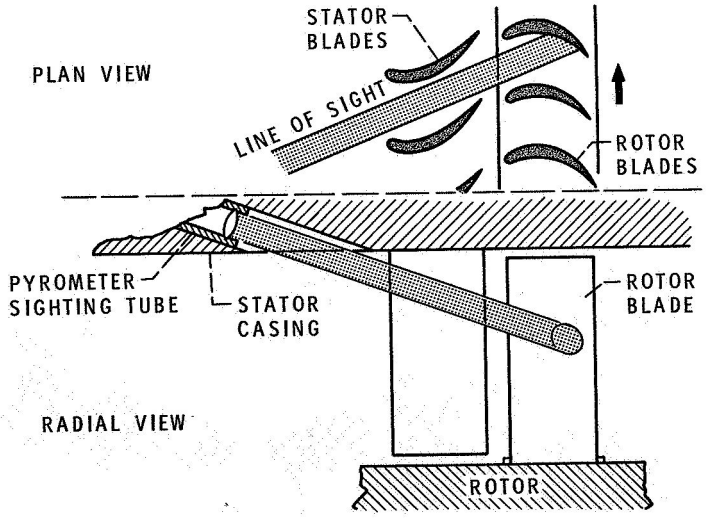

Figure 6-7. - Turbine-blade pyrometer installation.

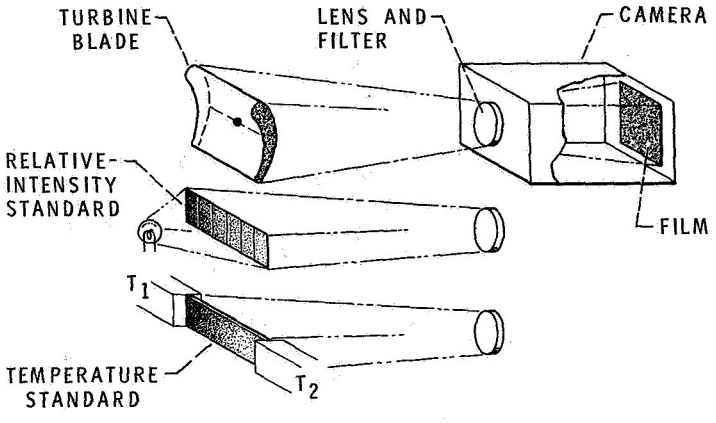

Figure 6-8. - Infrared temperature mapping. Stator blade.

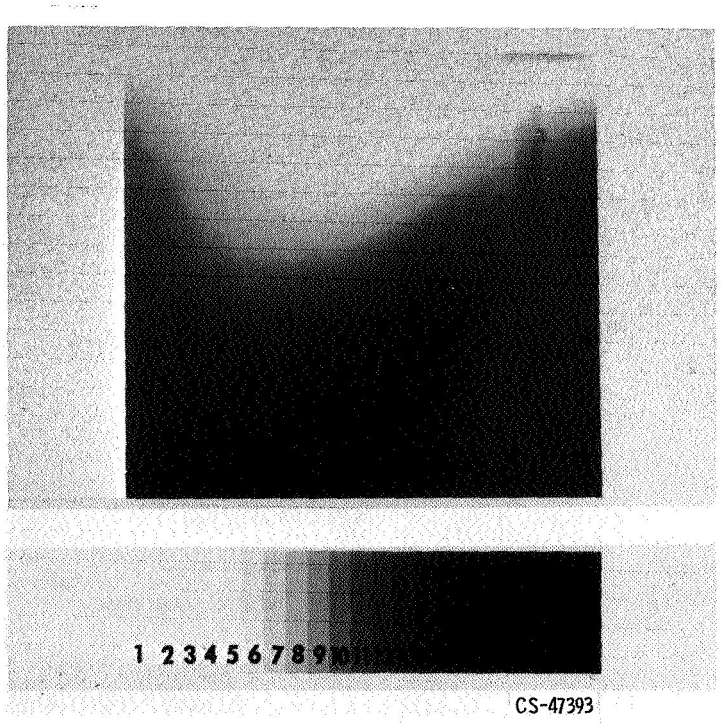

Figure 6-9. - Heated blade and relative intensity standard.

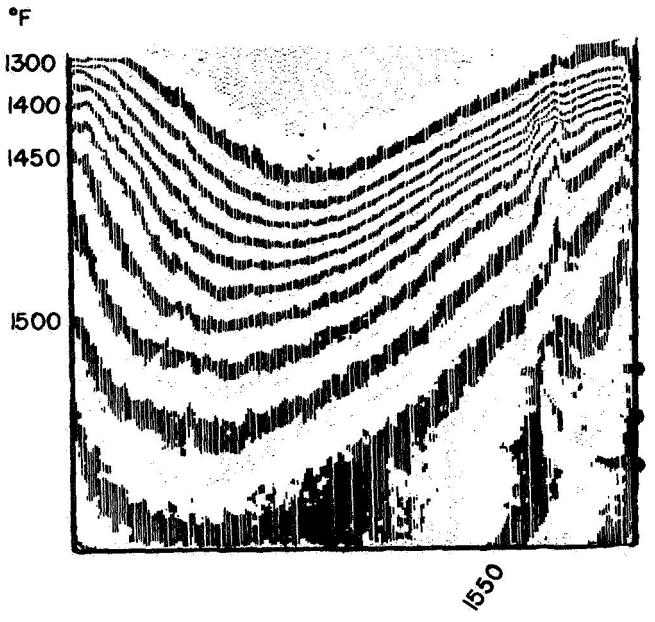

Figure 6-10. - Temperature contours on heated blade.

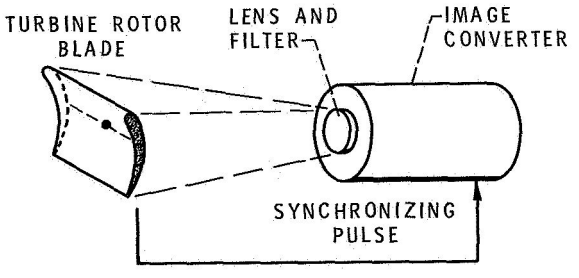

Figure 6-11. - Infrared temperature mapping. Rotor blade.

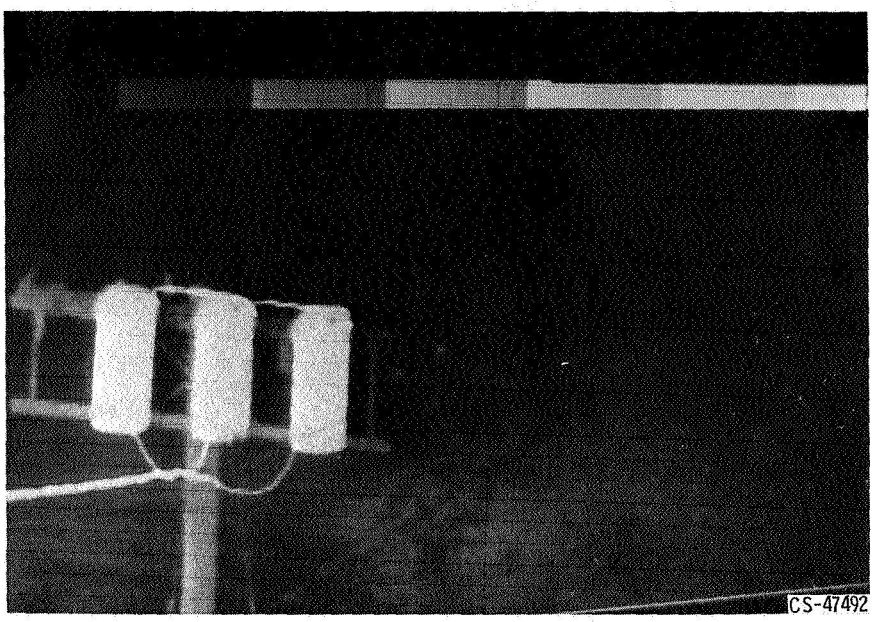

Figure 6-12. - Distribution transformers. (Courtesy Barnes Engineering Co.)

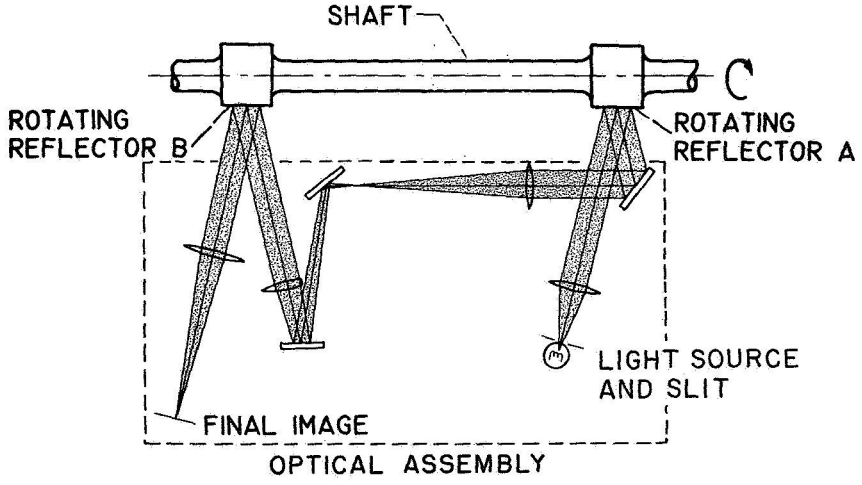

Figure 6-13. - Optical torquemeter.

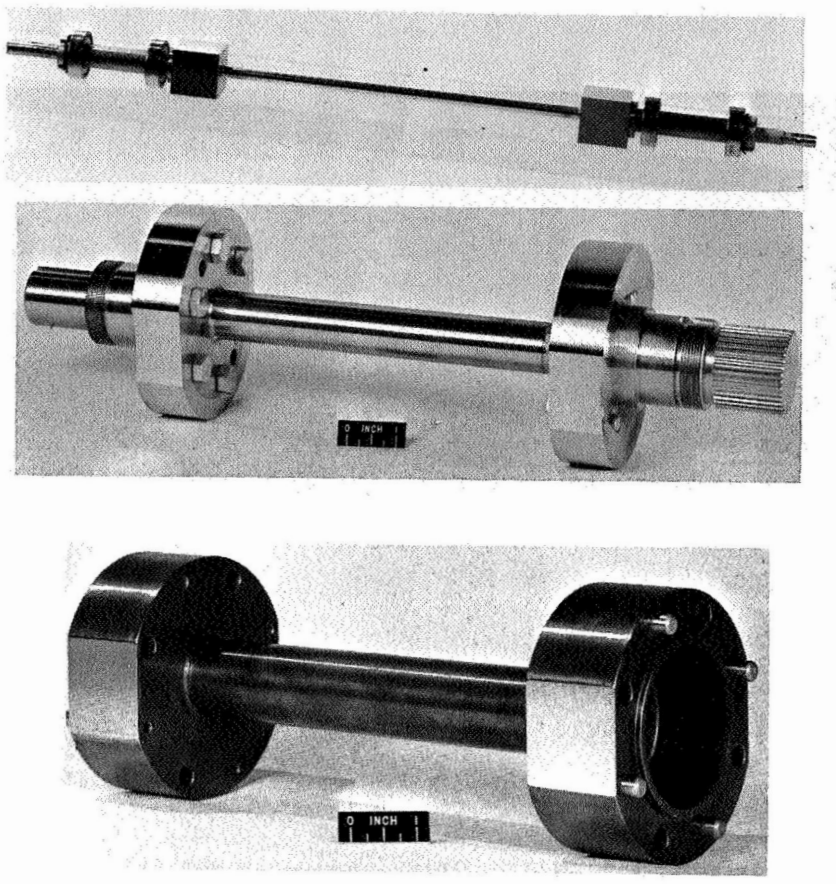

Figure 6-14. - Optical-torquemeter elements.

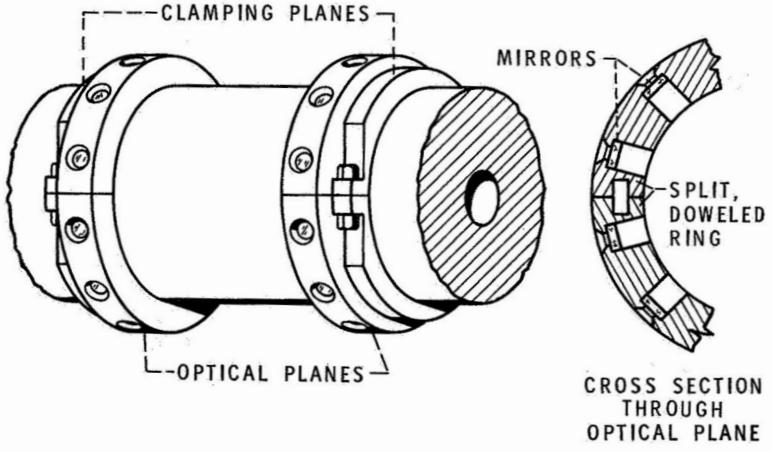

Figure 6-15. - Clamp-on optical-torquemeter element.

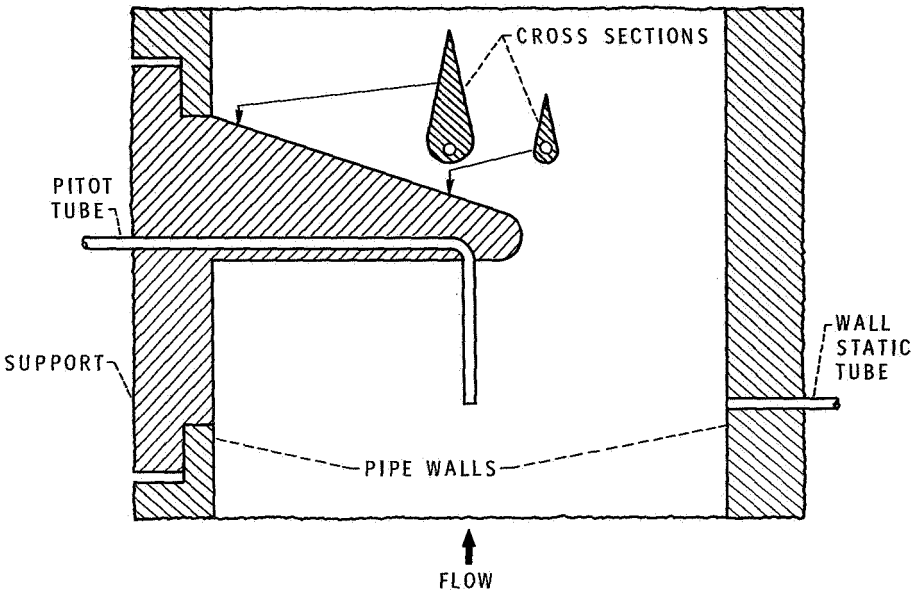

Figure 6-16. - Pitot tube.

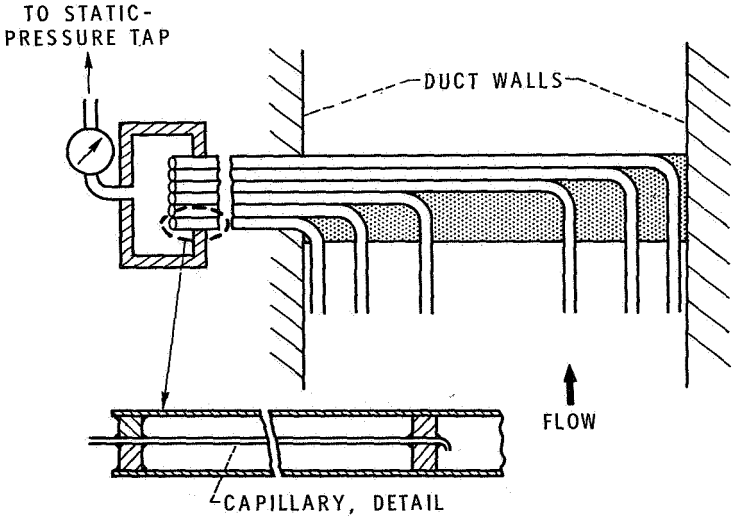

Figure 6-17. - Integrating rake.

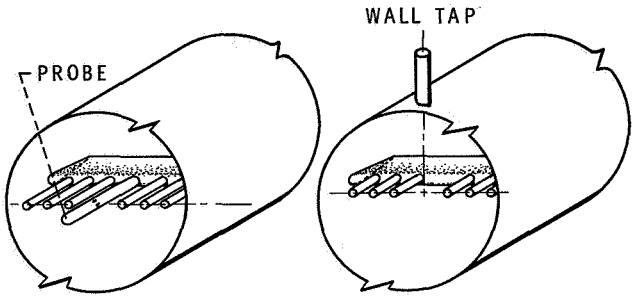

(a) Strut-mounted probe. (b) Wall tap.

Figure 6-18. - Static-pressure measurement.

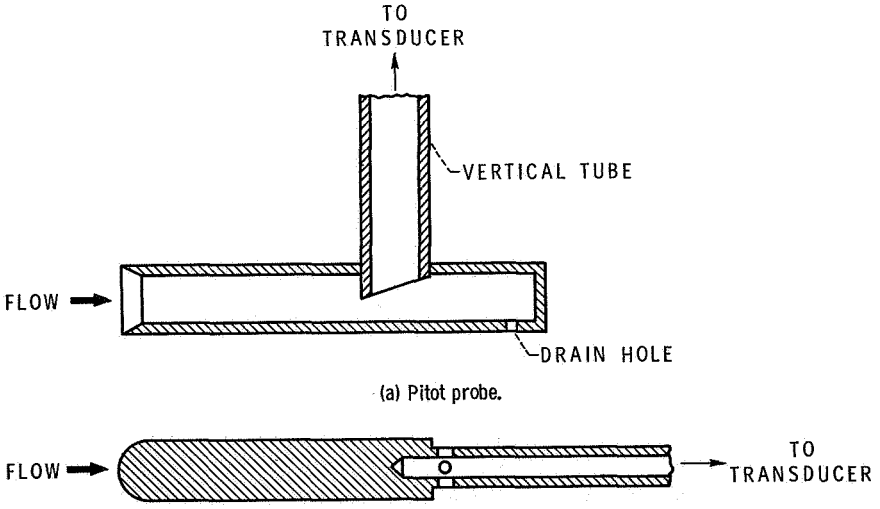

(a) Pitot probe.

(b) Static-pressure probe.

Figure 6-19. - Inertial separation of droplets.

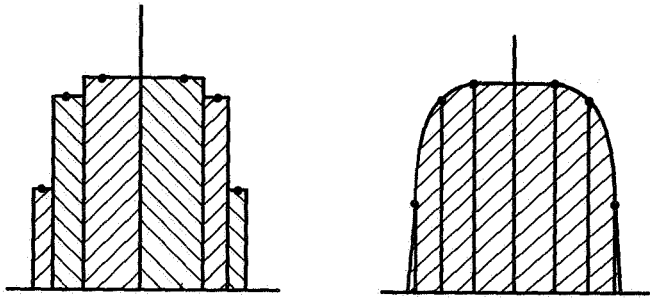

(a) Summation of areas.

(b) Summation with smoothing (Chebyshef integration).

Figure 6-20. - Integration by sampling.

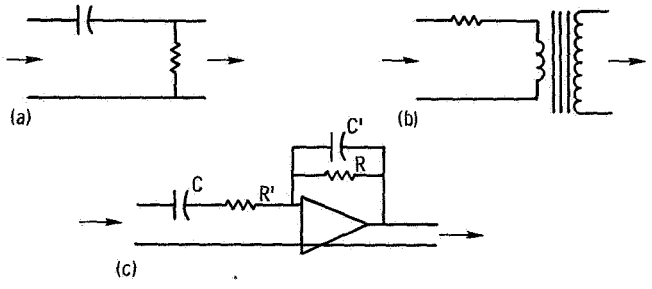

(a) Basic resistance-capacitance network.

(b) Basic resistance-inductance network with transformer.

(c) Practical resistance-capacitance network with operational amplifier.

Figure 6-21. - Rate indicators.

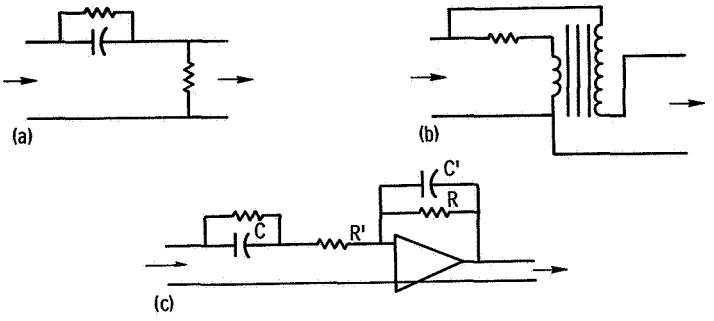

(a) Resistance-capacitance type.

(b) Transformer type.

(c) Practical resistance-capacitance type using operational amplifier.

Figure 6-22. - Time-lag compensators.

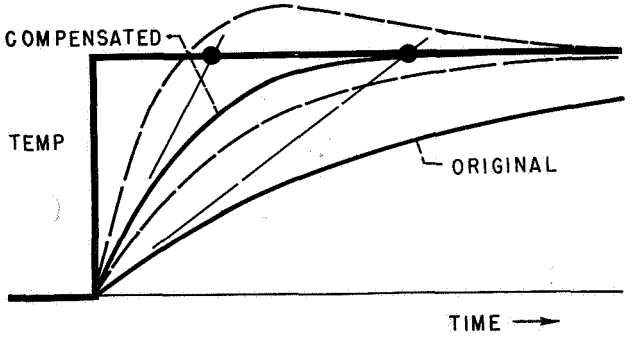

Figure 6-23. - Time-lag compensation.

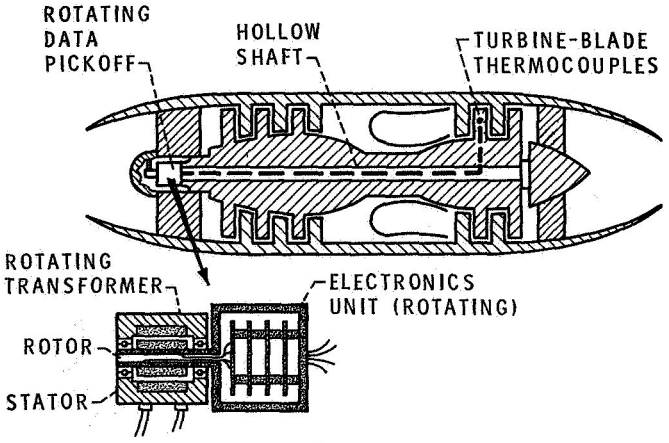

Figure 6-24. - Rotating-shaft data transmission.

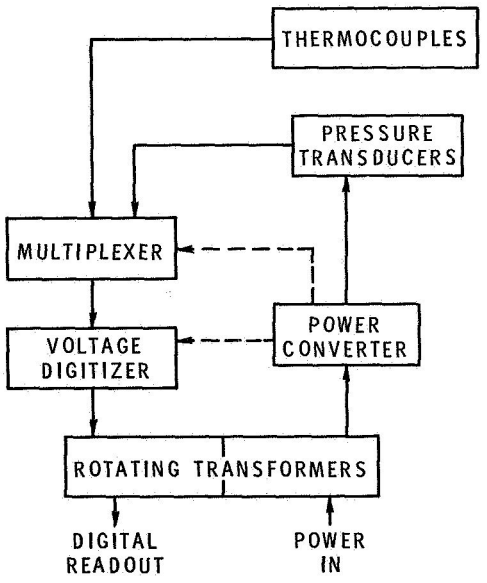

Figure 6-25. - Block diagram of rotating-shaft data transmission system.

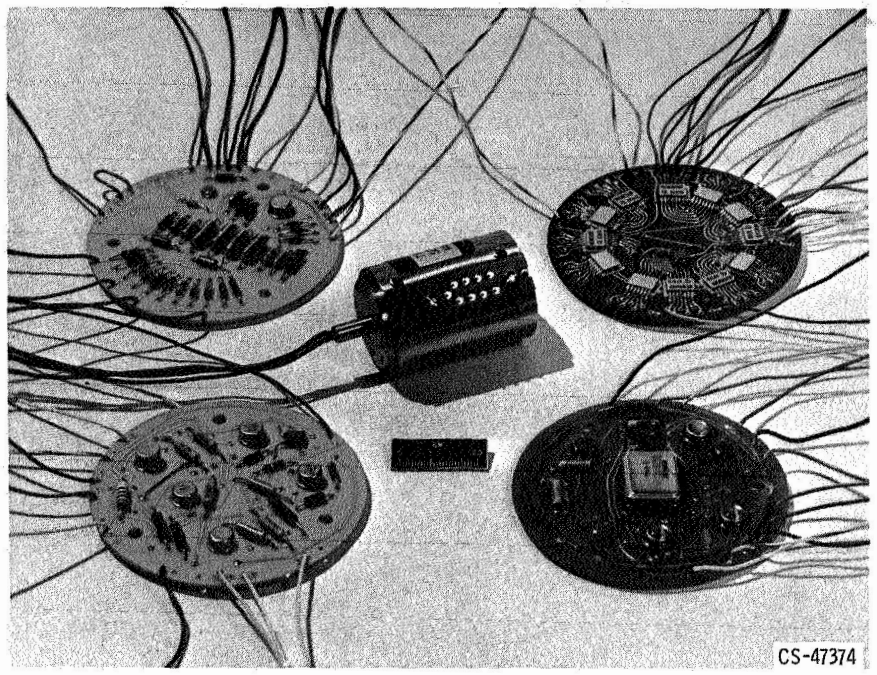

Figure 6-26. - Components of rotating-shaft data transmission system.